



Field emission properties of different forms of carbon

Vladimir I. Merkulov^{a,*}, Douglas H. Lowndes^a, Larry R. Baylor^a, Sukill Kang^b

^a Oak Ridge National Laboratory, Solid State Division, Building 3150, MS 6056, Oak Ridge, TN 37831-6056, USA

^b Department of Physics and Astronomy, University of Tennessee, Knoxville, TN 37996, USA

Abstract

The results of field emission (FE) studies are reported for three different forms of carbon: smooth amorphous carbon (a-C) films with both low and high sp^3 content prepared by pulsed-laser deposition (PLD), nanostructured carbon prepared by hot-filament chemical-vapor deposition (HFCVD), and vertically aligned carbon nanofibers (VACNFs). The studies reveal that smooth PLD carbon films are poor field emitters regardless of their sp^3 content. Conditioning of the films, which resulted in films' modification, was required to draw FE current and the emission turn-on fields were relatively high. In contrast, HFCVD carbon films exhibit very good FE properties, including low-emission turn-on fields, relatively high emission site density, and excellent durability. Finally, VACNFs also were found to possess quite promising FE properties that compete with those of HFCVD films. We believe that the latter two forms of carbon are among the most promising candidates for use as cold cathodes in commercial devices. © 2001 Elsevier Science Ltd. All rights reserved.

Keywords: Field emission; Diamond; Amorphous carbon; Carbon nanotubes and nanofibers; Nanostructure

1. Introduction

Electron field emission (FE) from various carbon (C)-based materials has been of substantial interest to the industrial and scientific communities worldwide, as potential applications of these materials in cold cathodes for FE displays and other vacuum microelectronic devices appear feasible [1–3]. Materials such as “coral-like” C [4], chemical-vapor deposited (CVD) diamond [5], shock-synthesized nanodiamond [6], carbon nanotubes (CNTs) (see e.g. Refs. [7,8] and references therein), CVD nanostructured C [9], and hot-filament (HF) CVD C [10] all were shown to exhibit very encouraging FE characteristics. In particular, very low-FE threshold fields were observed for these materials. Of course, for practical emitters other criteria such as high emission site density (ESD), good stability, and long

lifetime also must be considered, since these are crucial for actual device performance. The emission mechanism for the C-based materials is not completely understood but seems to involve a substantial geometrical enhancement factor (GEF) for the local electric field, due to nanoscale surface morphology, electron tunneling through the adsorbate states, and perhaps electric field enhancement created by highly non-uniform electronic properties over short (nanometer) distances.

Despite the fact that FE from C films has been under intense investigation by numerous research groups, many published studies are misleading or incomplete. Furthermore, novel materials such as various forms of nanostructured C have emerged. Their potentially promising FE properties are of great interest but have not yet been thoroughly studied and reported. In this paper we summarize the results of our comparative FE studies of three forms of C:

(i) *Smooth amorphous carbon films with variable sp^3 content:* The results reported in the literature are mixed, with some researchers finding that C films with high fractions of sp^3 -bonded C atoms exhibit very good FE properties [11], while others [4,10,12,13] do not.

* Corresponding author. Tel.: +1-865-241-1598; fax: +1-865-576-2813.

E-mail address: merkulovvi@ornl.gov (V.I. Merkulov).

(ii) *Nanostructured C prepared by hot-filament chemical-vapor deposition (HFCVD)*: This form of C seems quite promising for FE applications as it satisfies practically all of the cold cathode requirements outlined above. In particular, low-FE turn-on fields and relatively high ESD are observed, which we attribute to the material's nanostructure that is created during the deposition process.

(iii) *"Forests" of vertically aligned (perpendicular to the substrate) carbon nanofibers (VACNFs)*: To date, very few FE studies of this interesting material were reported in the literature [14,15], although there is a great number of FE studies of either individual CNTs or "mats" of non-aligned, "spaghetti-like" CNTs.

At first sight, FE tests seem relatively simple to perform but this is quite far from reality. The problem lies in the fact that the FE properties of materials can be drastically affected by a number of factors, most of which are rather difficult to monitor during the measurements. Consequently, accurate interpretation of FE results is often problematic. The most common parameter used to interpret FE results is the work function (WF) or electron affinity (EA) of a large, relatively smooth and clean surface of a material studied. However, it is *not the only*, and in many cases *not the dominant*, parameter governing FE. Several other factors can play an extremely important role. First, surface contamination such as various adsorbates from the ambient atmosphere as well as surface oxides can change the height and the width of the tunneling barrier at the surface and consequently the FE characteristics. Second, particles and protrusions are typically always present on the surface and can drastically alter the local GEF and therefore FE. Finally, FE measurements are destructive in nature. Consequently, materials being tested can be modified during the measurements. This is manifested in modifications of both the surface morphology and the WF/EA. All of the above parameters are crucial for the correct interpretation of FE results but unfortunately are often neglected.

An experimental setup that is frequently used for FE measurements is a non-imaging parallel plate anode separated from the cathode (the sample) by dielectric spacers. This method has a major flaw of measuring FE from the sample's "hottest" (most easily emitting) spots *only*. It completely fails to determine ESD (the number of emitting sites per unit area at a given applied field) which is a crucial parameter for elucidating FE mechanisms and for fabricating actual devices. The hottest spots can easily be particles, protrusions (highly locally enhanced GEF) or regions of modified or contaminated material (altered GEF and WF/EA) and therefore will not represent the bulk material being tested. In addition, in the parallel-plate method the leakage current across the spacers separating the anode from the sample is rather difficult to distinguish from the true FE current.

This is why we believe that the non-imaging parallel plate method provides no reliable information about the average FE properties of a thin-film material over large surface areas. FE is a *local* phenomenon and therefore local probes such as a sharp scanned probe with three translational degrees of freedom or/and an imaging screen should be used as the anode for FE measurements. In addition, FE energy distribution (FEED) measurements [16] can be particularly useful for elucidating FE mechanisms. In our lab we use a scanned probe, and the results and analysis of FE measurements utilizing this technique are discussed below.

2. Experimental

The detailed description of materials preparation can be found elsewhere [10,17,18]. Briefly, the deposition conditions and characterization techniques for various C materials were as follows. Pulsed-laser deposited (PLD) amorphous C films with systematically variable sp^3 bonding, ranging from highly tetrahedral amorphous C (ta-C, up to $\sim 75\%$ sp^3 -bonded C atoms) to predominantly sp^2 -bonded a-C, were formed by ablation of a graphite target in a high vacuum chamber (base pressure of 3×10^{-8} Torr) using a Lambda Physik Compex 301i pulsed excimer laser operated with ArF (193 nm). The sp^3 content was measured by electron energy loss spectroscopy (EELS) as described previously [17]. Hot-filament chemical vapor deposition (HFCVD) C was deposited in a vacuum chamber with a base pressure $< 1 \times 10^{-7}$ Torr. A tungsten filament was placed a few mm above the sample. Ethylene (C_2H_4) was used as a C gas source and was directed onto the hot filament using a stainless steel nozzle. The chamber pressure during the deposition was 1.2×10^{-4} Torr. The sample temperature varied between $570^\circ C$ and $750^\circ C$, depending upon the distance between the filament and the sample, and was measured by a thermocouple attached directly to the sample surface. For both the PLD and HFCVD films n-type Si wafers were used as substrates.

VACNFs were prepared by a method similar to that used by Ren et al. [19]. The method utilizes plasma-enhanced CVD in a vacuum chamber evacuated by a mechanical pump to a base pressure $< 5 \times 10^{-3}$ Torr. The substrates were fabricated by evaporating a thin layer (~ 10 nm) of Ni catalyst onto an n-type Si wafer that had been pre-coated with 100 nm of W or W-Ti, to prevent formation of Ni silicide at elevated temperatures. Upon plasma pre-etching and heating the substrates above $\sim 600^\circ C$, the Ni layer breaks into little droplets that are the necessary precursors for the catalytic growth of VACNFs [18]. Acetylene (C_2H_2) and a mixture of 10% ammonia (NH_3) and 90% helium (He), with gas flows of 15 and 200 sccm correspondingly, were used as the gas source. NH_3 is needed to etch away a thick graphitic C

film that continuously forms during the growth from the plasma discharge and passivates the Ni catalyst, thereby preventing the formation of CNFs. The NH_3/He mixture was introduced into the chamber first and the plasma was started; after that the C_2H_2 was introduced. The typical pressure during the growth was several Torr, the substrate temperature was $\sim 700^\circ\text{C}$, and the plasma discharge was operated at 50–100 mA and ~ 500 V.

To obtain structural information, Raman scattering measurements were done using a Lexel 3500 Ar ion laser operating at 514.5 nm and a Dilor XY Raman spectrometer equipped with a EG&G OMA 4 CCD detector. Surface morphology studies were performed utilizing a Philips XL30/FEG high resolution scanning electron microscope (HRSEM) with X-ray energy dispersive spectroscopy (EDS) capabilities and a Nanoscope IIIa (Digital Instruments) atomic force microscope (AFM) that was operated in tapping mode.

FE measurements were carried out in a high vacuum chamber with a base pressure of 10^{-6} Torr. The measurements were taken by applying a positive voltage to a tungsten current probe (anode) and by collecting electrons emitted from the sample (cathode). Current probes' tips were approximately spherical with diameters (twice the radius of curvature) ranging from 1 to 25 μm . The probe tip roughness was on a deep submicron level as verified by HRSEM measurements. The typical distance between the probe and the samples during the measurements was 5–20 μm . The turn-on field remained essentially constant within this distance range. To obtain better statistics each sample with a typical size of $\sim 1 \times 1$ cm^2 was measured at several different locations separated from one another by a few mm. 2D scans of FE turn-on field were performed periodically over a typical sampling area of $\sim 200 \times 200$ μm^2 . The current probe stage motion was computer controlled with the minimum step size of 75 nm in x – y – z directions, which allowed for precise control of the probe position.

3. Results and discussion

3.1. Smooth amorphous C films

For all of the PLD amorphous C samples tested, regardless of their sp^3 content, the “conditioning” process [12,13] was required to obtain any measurable emission. Conditioning typically resulted in arcing that occurred between the probe and the sample as the electric field was increased from 0 to 100–200 $\text{V}/\mu\text{m}$. After the conditioning, a typical turn-on field required to draw ~ 1 nA FE current from highly (up to $\sim 75\%$) sp^3 -bonded C films (ta-C) was ~ 50 $\text{V}/\mu\text{m}$ which is substantially higher than for other forms of carbon [4–10]. A typical emission current-applied electric field (I – E)

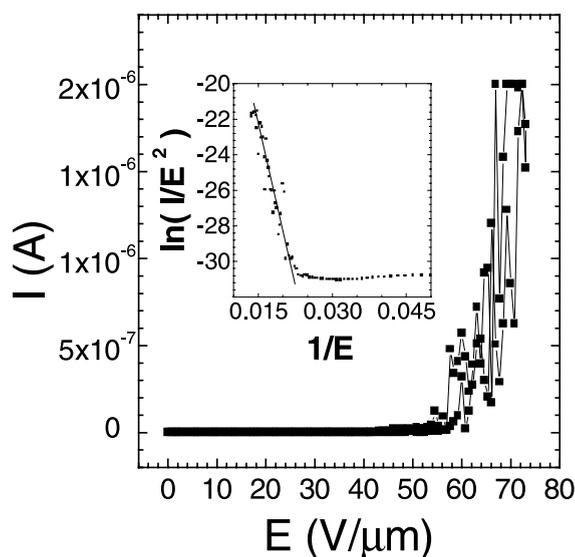


Fig. 1. Emission current-applied electric field (I – E) curve and Fowler–Nordheim plot (inset) for $\sim 73\%$ sp^3 ta-C film after conditioning.

curve for these films after the conditioning process is shown in Fig. 1. The macroscopic electric field, E , was simply calculated as the probe voltage divided by the probe–sample distance. As the probe was moved to a new location the emission vanished and conditioning was required again to restart it. After moving the probe back to the previously conditioned spot the emission would resume with no additional conditioning required. Further, we found that conventional predominantly sp^2 -bonded a-C, prepared by PLD with low C-ion kinetic energies, exhibited very similar FE characteristics but perhaps with somewhat lower fluctuations of the emission current. The emission curves were similar for both high and low sp^3 content PLD films and followed the Fowler–Nordheim (FN) behavior over part of the I – E plot, as shown in the inset of Fig. 1. Using a simplified FN equation [20] and assuming the WF of amorphous C films similar to that of graphite ($\Phi \sim 4.6$ eV), it is possible to roughly estimate the emitting area and the geometric enhancement factor (β) of the electric field due to sample’s local surface morphology. The calculations yield low-emitting area $\sim 10^{-2}$ μm^2 and high $\beta \sim 100$ – 150 for both ta-C and sp^2 -bonded a-C films, contradictory to our AFM measurements which show that the as-deposited films are extremely smooth [21], with rms roughness ~ 1 – 2 Å. Of course, the WF/EA of the PLD C films may differ from that of graphite. Therefore, even a smooth film could, in principle, emit at low applied fields if the WF/EA were very low. Although we note that it must be almost unrealistically low (< 0.3 eV) for emission to occur from a perfectly smooth surface.

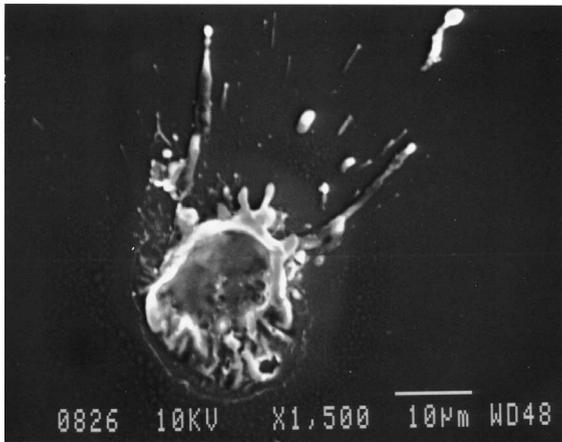


Fig. 2. SEM image of a crater formed as a result of the conditioning process (arc discharge) of initially smooth amorphous C film.

To further investigate this issue, SEM was employed to study changes in surface morphology that occurred after the arcing. The measurements revealed that at the location of severe arcing, where the initial film was smooth, a crater of once-molten C film and Si substrate was formed (see Fig. 2). Given this fact and the FE characteristics of ta-C films described above, we conclude that FE from ta-C is not due to low WF/EA but rather should be attributed to the sharp protrusions around the crater formed during the arcing. The protrusions geometrically enhance the electric field, thereby providing for electron emission at moderate fields. We note that there may be another factor contributing to low-FE turn-on fields: the formation of small sp^2 regions embedded into the sp^3 matrix, which occurs during even the “gentle” conditioning process [22]. The applied electric field can be greatly enhanced at the conductive sp^2 regions, promoting electron emission from these regions at relatively low applied fields [23].

We also note that our very first FE measurements of ta-C films were performed using a non-imaging parallel-plate method and the measured turn-on fields were found to be only ~ 5 V/ μm . This demonstrates again that the parallel plate method can be quite deceiving and is unreliable in general for the reasons discussed in the introduction.

3.2. Hot-filament chemical-vapor deposited carbon

As-deposited HFCVD films are thoroughly nanostructured. A typical high resolution SEM image is shown in Fig. 3. “Bumps” of a few hundred nm in size are observed. The bumps seem to be composed of very fine features that cannot be clearly resolved by HRSEM.

The measured Raman spectra (see Fig. 4) exhibited two broad peaks located at ~ 1350 and 1600 cm^{-1} . This is characteristic of graphitic, nanocrystalline C with a grain size < 25 Å [24]. Surprisingly, EDS measurements also revealed the presence of Ni in the films. It was found that the W wire that we used for making filaments contained a small amount ($\sim 1\%$) of Ni. As a result, a thin (~ 80 nm) layer of Ni was deposited within the first minute of the filament being turned on and only after that the C film was formed. W filaments without Ni did not produce any C films under the otherwise identical experimental conditions. We conclude that nanostructured, predominantly sp^2 -bonded C films formed due to the catalytic growth reaction between Ni and C_2H_4 , which is probably similar to the growth process of car-

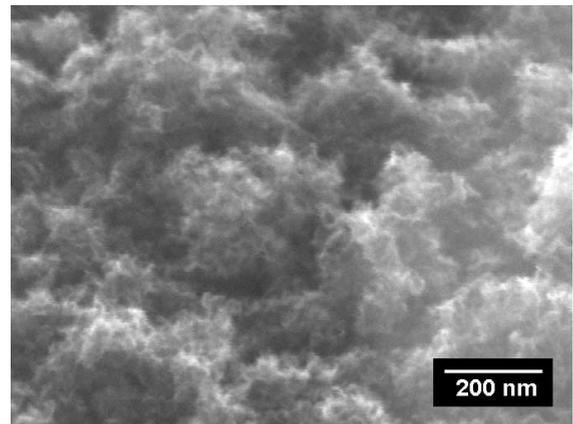


Fig. 3. High resolution SEM image of HFCVD C taken at 15 kV and 50° tilt angle. The image shows nanostructured nature of HFCVD C films.

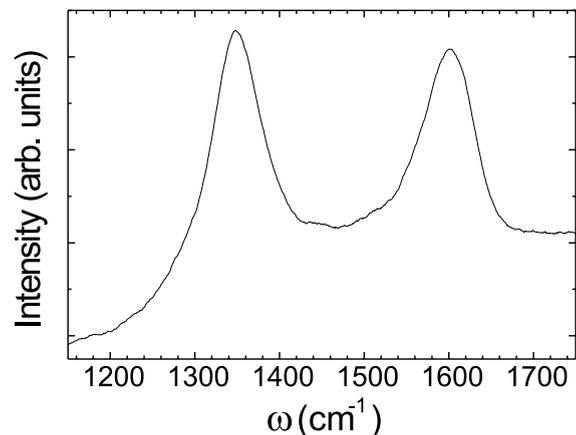


Fig. 4. Raman spectrum of HFCVD C. The two peaks located at ~ 1350 and 1600 cm^{-1} are representative of the sp^2 -bonded, nanocrystalline structure.

bon fibers [25]. We note that the possibility of the presence of small diamond nanocrystallites in the films cannot be completely ruled out at this point, since Raman scattering in the visible would not be able to detect small amounts of sp^3 -bonded C due to the low cross-section of the sp^3 -bonding in the visible. UV Raman scattering [26,27] accompanied by high resolution transmission electron microscopy (HRTEM) and EELS would be necessary to characterize HFCVD C more completely. However, we do not believe that sp^3 crystallites are very likely to be present in these films since the growth temperature was too low for the diamond formation and no special substrate treatment was employed. Furthermore, even if occasional diamond crystallites were nevertheless present in the films they would most likely be covered with a thick layer of sp^2 carbon and therefore would not affect FE process to any substantial degree. As a result, we do not consider diamond crystallites in the discussion of the FE mechanism, although further structural characterization of the HFCVD films is definitely needed.

HFCVD C films were found to exhibit very promising FE characteristics. First, no conditioning or arcing was required to initiate emission once the threshold field was reached, and no substantial hysteresis was observed, which suggests a non-destructive FE mechanism. Second, the turn-on fields were quite low and varied from 7 to 30 $V/\mu m$ depending upon the deposition conditions and the location on the sample. We also note that films deposited at higher temperatures tended to exhibit lower turn-on fields along with more extensive nanostructure. Third, when the probe was scanned across the sample surface the ESD was found to be high. An example of a 2D ($200 \times 200 \mu m^2$) scan is shown in Fig. 5. The sample emitted continuously across the surface, although the FE turn-on field varied from 9 to 15 $V/\mu m$. If one assumes that the only emitting surface is located under the probe, then the resolution is limited only by the probe diameter ($\sim 1 \mu m$) and the ESD at 15 $V/\mu m$ is at least $\sim 1 \text{ site}/(1 \mu m)^2 \sim 1 \times 10^8 \text{ sites}/cm^2$. This would more than satisfy the most severe requirements for FE displays. However, due to the variation in the turn-on field across the sample surface, the areas with lower turn-on fields may emit even if they are not located directly under the probe. It appears from Fig. 5 that there may be low-turn-on-field emitting spots at intervals of a few tens of μm , and the current probe is simply activating only these sites as it scans over them. Considering the distance between the probe and the sample surface (20 μm) and the variation of the turn-on field (9–15 $V/\mu m$) a more conservative estimate of the ESD yields at least $\sim 1 \text{ site}/(25 \mu m^2) = 1.6 \times 10^5 \text{ sites}/cm^2$, which is a substantially smaller number but nevertheless is still suitable for lower resolution displays.

The material was also found to be very robust. The maximum current obtained before damaging the sam-

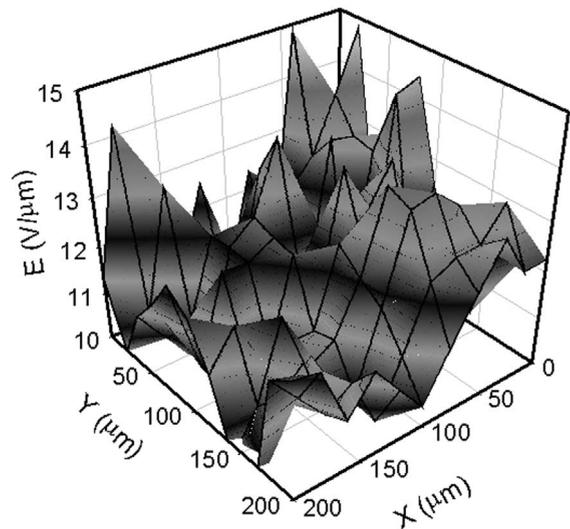


Fig. 5. Emission turn-on field, defined as the field required to draw 1 nA of emission current to the probe, as a function of the probe position in the HFCVD C sample plane. The distance between the probe and the sample is 20 μm .

ple was $\sim 5\text{--}50 \mu A$ for a 20 μm diameter probe that was positioned directly above the locations with lower turn-on fields. In this case it is reasonable to assume that only the area under the probe is emitting, which yields a macroscopic current density of at least $\sim 1\text{--}10 A/cm^2$ which is at least 10–100 times higher than that required for FED applications. Finally, our preliminary results show that the emission is stable for at least 30–50 h. Mechanical instabilities (probe drift) in our system precluded longer measurements of the emission lifetime.

We attribute the promising FE characteristics of HFCVD C mainly to its nanostructure and associated with it high GEF. Due to the sp^2 nature of this material, the WF should be relatively large (a few eV) resulting in very high extracting fields for a flat surface. However, as can be seen from Fig. 3 the bumps on the sample surface are a few hundred nm tall and if the nanoprotusions have nanometer and subnanometer thickness (a stack of a few graphitic planes) the GEF required to account for the low-turn-on fields can be easily achieved. Unfortunately, HRSEM resolution is not sufficient to accurately determine the aspect ratio (AR) of the HFCVD nanostructure, although features below 10 nm in size are definitely observed. Again, HRTEM is required for better characterization of this material.

There are a few other possible factors that may contribute to the improved FE properties. They include elastic resonant tunneling through virtual energy levels of adsorbates on the surface that can substantially increase the FE tunneling probability [16] and drastic changes of the electronic structure, such as a semimetal-to-semiconductor phase transition [28] and the presence

of narrow energy bands above the Fermi level [29], as the size of graphitic clusters decreases. More studies and in particular FEED measurements [16] are needed to differentiate between these possibilities.

3.3. Vertically-aligned carbon nanofibers

The FE turn-on fields for the forests of VACNFs were found to depend on several parameters including the VACNF AR, the height variation, and the nucleation site density. Very dense forests (40–60 nanofibers/ μm^2) with relatively small ($\sim 20\%$) height variation exhibited quite high FE turn-on fields, $>100 \text{ V}/\mu\text{m}$. In fact, in most cases arcing occurred before the required threshold field was achieved. This was the case even for the forests of VACNFs with high ARs >200 . However, assuming the CNF WF similar to that of graphite as an approximation and employing the FN equation, the turn-on fields are expected to be of the order of $\sim 15\text{--}25 \text{ V}/\mu\text{m}$. We conclude that the reason for the virtual absence of FE from dense forests of VACNFs, even at high electric fields, is the screening of the electric field at the ends of VACNFs by the neighboring nanofibers, which occurs when they are placed too close to each other. Dense VACNF forests and smaller height variation result in reduced enhancement of the local electric field at each nanofiber tip. Similar effect was reported recently by Nilsson et al. [30] for films of non-oriented, spaghetti-like CNTs.

For relatively sparse VACNF forests ($\leq 10 \text{ VACNFs}/\mu\text{m}^2$), such as the one shown in Fig. 6, FE characteristics were found to be substantially improved. No conditioning was required to initiate FE and emission was continuous as the probe was scanned across the sample surface. The turn-on fields ranged from 13 to $30 \text{ V}/\mu\text{m}$. A typical 2D scan with a $1 \mu\text{m}$ diameter probe is

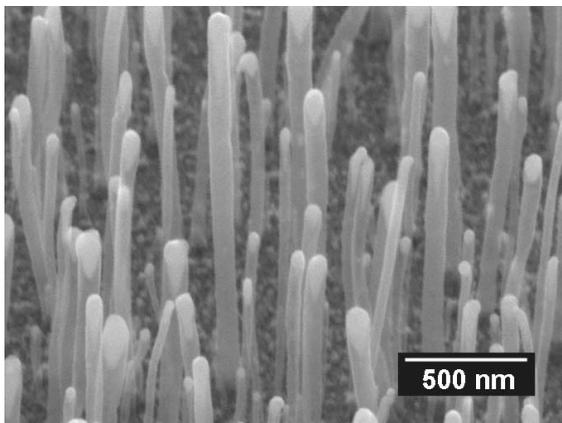


Fig. 6. High resolution SEM image of a sparse forest of vertically aligned carbon nanofibers. The image is taken at 15 kV and 50° tilt angle.

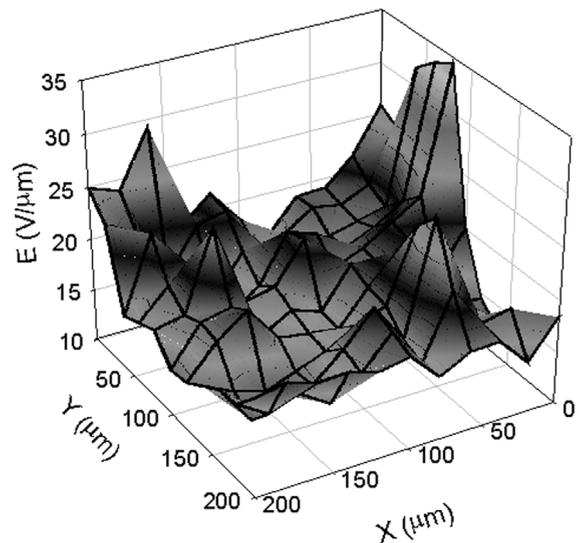


Fig. 7. 2D scan of the field emission turn-on field for vertically aligned carbon nanofibers. The distance between the probe and the sample is $20 \mu\text{m}$ and the FE current to the probe was 1 nA .

shown in Fig. 7. Similar to the discussion of HFCVD C, the optimistic estimate of the ESD at $30 \text{ V}/\mu\text{m}$ is $\sim 1 \text{ site}/(1 \mu\text{m})^2 \sim 1 \times 10^8 \text{ sites}/\text{cm}^2$, whereas the conservative one yields at least $\sim 1 \text{ site}/(40 \mu\text{m})^2 \sim 6 \times 10^4 \text{ sites}/\text{cm}^2$. We note that the CNF AR in this case is only $\sim 50 \pm 10$ and, even in the complete absence of screening, turn-on fields substantially (two to three times) higher than $15\text{--}30 \text{ V}/\mu\text{m}$ are expected. In fact, turn-on fields should be even higher since substantial screening is supposed to be present even in these sparse forests of VACNFs according to the calculations by Nilsson et al. [30]. We speculate that nanometer- and subnanometer-scale roughness of the VACNF tip contribute additional enhancement of the electric field. Theoretical calculations performed for a blunt tip with a small bump on its apex show that the GEF can be enhanced by up to a factor of 3 due to the bump [31], which would account at least partially for the lower-than-expected turn-on fields. Also, elastic-resonant and inelastic tunneling through the adsorbate states and possibly additional non-metallic states above the Fermi level at the nanofiber tips [32,33] are likely to be among the contributing factors.

Preliminary FE stability tests show that electron emission from VACNFs is likely to have a long lifetime. An emission current of 100 nA on the probe was maintained for at least 150 h , the longest time for which measurements were done. The maximum FE current before VACNF damage occurred was at least $7 \mu\text{A}$ for a $1 \mu\text{m}$ diameter probe, corresponding to a macroscopic current density of $\sim 900 \text{ A}/\text{cm}^2$ for the VACNF film, and an estimated current density of $\sim 35\text{--}350 \text{ kA}/\text{cm}^2$ per VACNF tip, depending on how many nanofibers under

the 1 μm probe are emitting. This is in good agreement with observations by Baker et al. [34] for individual carbon-fiber field emitters.

4. Conclusions

In conclusion, we have investigated the FE properties of smooth carbon films with both high and low sp^3 fraction, nanostructured HFCVD carbon, and carbon nanofibers well-aligned in the direction perpendicular to the substrate (VACNFs). While smooth carbon films are not good field emitters, both HFCVD C and VACNFs exhibit very promising FE characteristics, such as the absence of conditioning, low-turn-on fields, relatively high ESD, and durability. Nanostructure and high enhancement of the extracting local electric field associated with it, as well as various mechanisms of reduction of the tunneling barrier at the surface, are believed to be responsible for such promising FE characteristics.

Acknowledgements

We are grateful to E.A. Kenik and the SHaRE facility for providing the microscope for SEM measurements. We also thank P.H. Fleming for assistance with sample preparation. This research was conducted at Oak Ridge National Laboratory (ORNL), with support from DARPA/MTO under contract no. 1868HH26X1 and from the ORNL LDRD program. ORNL is managed by UT-Battelle, LLC, for the US Department of Energy under contract no. DE-AC05-00OR22725.

References

- [1] Choi WB, Chung DS, Kang JH, Kim HY, Jin YW, Han IT, Lee YH, Jung JE, Lee NS, Park GS, Kim JM. Fully sealed, high-brightness carbon-nanotube field-emission display. *Appl Phys Lett* 1999;75(20):3129–31.
- [2] Saito Y, Mizushima R, Tanaka T, Tohji K, Uchida K, Yumura M, Uemura S. Synthesis, structure, and field emission of carbon nanotubes. *Fuller Sci Technol* 1999;7(4):653–64.
- [3] Wang QH, Setlur AA, Lauerhaas JM, Dai JY, Seelig EW, Chang RPH. A nanotube-based field-emission flat panel display. *Appl Phys Lett* 1998;72(22):2912–3.
- [4] Coll BF, Jaskie JE, Markham JL, Menu EP, Talin AA, von All P. Field emission properties of disordered and partially ordered clustered carbon films. In: Siegal MP, Milne WI, Jaskie JE, editors. *Covalently bonded disordered thin-film materials*. Mater Res Soc Proc, Warrendale, 1998. p. 185–95.
- [5] Zhou D, Krauss AR, Corrigan TD, McCauley TG, Chang RPH, Gruen DM. Microstructure and field emission of nanocrystalline diamond prepared from C60 precursors. *J Electrochem Soc* 1997;144(8):224–8.
- [6] Zhu W, Kochanski GP, Jin S. Low-field electron emission from undoped nanostructured diamond. *Science* 1998;282:1471–3.
- [7] Bonard J-M, Salvétat J-P, Stockli T, Forro L, Chatelain A. Field emission from carbon nanotubes: perspectives for applications and clues to the field emission mechanism. *Appl Phys A* 1999;69:245–54.
- [8] Zhu W, Bower C, Zhou O, Kochanski G, Jin S. Large current density from carbon nanotube field emitters. *Appl Phys Lett* 1999;75(6):873–5.
- [9] Obratsov AN, Volkov AP, Pavlovskii IYu, Chuvilin AL, Rudina NA, Kuznetsov VL. Role of the curvature of atomic layers in electron field emission from graphitic nanostructured carbon. *JETP Lett* 1999;69(5):411–7.
- [10] Merkulov VI, Lowndes DH, Baylor LR. Field emission studies of smooth and nanostructured carbon films. *Appl Phys Lett* 1999;75(9):1228–30.
- [11] Satyanarayana BS, Hart A, Milne WI, Robertson J. Field emission from tetrahedral amorphous carbon. *Appl Phys Lett* 1997;71(10):1430–2.
- [12] Missert N, Friedmann TA, Sullivan JP, Copeland RG. Characterization of electron emission from planar amorphous carbon thin films using in situ scanning electron microscopy. *Appl Phys Lett* 1997;70(15):1195–997.
- [13] Groning O, Kuttel OM, Schaller E, Groning P, Schlapbach L. Vacuum arc discharges preceding high electron field emission from carbon films. *Appl Phys Lett* 1996;69(4):476–8.
- [14] Murakami H, Hirakawa M, Tanaka C, Yamakawa H. Field emission from well-aligned, patterned, carbon nanotube emitters. *Appl Phys Lett* 2000;76:1776–8.
- [15] Chen Y, Shaw DT, Guo L. Field emission of different oriented carbon nanotubes. *Appl Phys Lett* 2000;76:2469–71.
- [16] Gadzuk JW, Plummer EW. Field emission energy distribution. *Rev Mod Phys* 1973;45(3):487–547.
- [17] Merkulov VI, Lowndes DH, Jellison Jr GE, Puretzy AA, Geohegan DB. Structure and optical properties of amorphous diamond films prepared by ArF laser ablation as a function of carbon ion kinetic energy. *Appl Phys Lett* 1998;73(18):2591–3.
- [18] Merkulov VI, Lowndes DH, Wei YY, Eres G, Voelkl E. Patterned growth of individual and multiple vertically aligned carbon nanofibers. *Appl Phys Lett* 2000;76(24):3555–7.
- [19] Ren ZF, Huang ZP, Xu JW, Wang JH, Bush P, Siegal MP, Provencio PN. Synthesis of large arrays of well-aligned carbon nanotubes on glass. *Science* 1998;282:1105–7.
- [20] Spindt CA, Brodie I, Humphrey L, Westerberg ER. Physical properties of thin-film field-emission cathodes with molybdenum cones. *J Appl Phys* 1976;47(12):5248–63.
- [21] Lowndes DH, Merkulov VI, Pedraza AJ, Fowlkes JD, Puretzy AA, Geohegan DB, Gellison Jr GE. Surface engineering of silicon and carbon by pulsed laser ablation. In: Kumar A, Chung Y-W, Moore JJ, Smugeresky JE, editors. *Surface engineering: science and technology I*. The Minerals, Metals and Materials Society, 1999. p. 113–26.
- [22] Mercer TW, DiNaro NJ, Rothman JB, Siegal MP, Friedman TA, Martinez-Miranda LJ. Electron emission induced modifications in amorphous tetrahedral diamond-like carbon. *Appl Phys Lett* 1998;72(18):2244–6.

- [23] Ilie A, Ferrari AC, Yagi T, Robertson J. Effects of sp^{-2} -phase nanostructure on field emission from amorphous carbons. *Appl. Phys. Lett.* 2000;76(18):2627–9.
- [24] Nemanich RJ, Solin SA. First- and second order Raman scattering from finite-size crystals of graphite. *Phys Rev B* 1979;20(2):392–401.
- [25] Baker RTK. Catalytic growth of carbon filaments. *Carbon* 1989;27(3):315–23.
- [26] Merkulov VI, Lannin JS, Munro CH, Asher SA, Veerasamy VS, Milne WI. UV studies of tetrahedral bonding in diamondlike amorphous carbon. *Phys Rev Lett* 1997;78(25):4869–72.
- [27] Adamopoulos G, Gilkes KWR, Robertson J, Conway NMJ, Kleinsorge BY, Buckley A, Batchelder DN. Ultra-violet Raman characterisation of diamond-like carbon films. *Diam Rel Mater* 1999;8(2–5):541–4.
- [28] Lopinski GP, Merkulov VI, Lannin JS. Semimetal to semiconductor transition in carbon nanoparticles. *Phys Rev Lett* 1998;80(19):4241–4.
- [29] Purcell ST, Binh Vu Thien, Garcia N, Lin ME, Andres RP, Reifengerger R. Field emission from narrow bands above the Fermi level of nanometer-scale objects. *Phys Rev B* 1994;49(24):17259–63.
- [30] Nilsson L, Groening O, Emmenegger C, Kuettel O, Schaeller E, Schlapbach L, Kind H, Bonard J-M, Kern K. *Appl Phys Lett* 2000;76(15):2071–3.
- [31] Mesa G, Dobado-Fuentes E, Saenz JJ. Image charge method for electrostatic calculations in field-emission diodes. *J Appl Phys* 1996;79(1):39–44.
- [32] Fransen MJ, van Rooy ThL, Kruit P. Field emission energy distribution from individual multiwalled carbon nanotubes. *Appl Surf Sci* 1999;146:312–27.
- [33] Dean KA, Groening O, Kuttel OM, Schlapbach L. Nanotube electronic states observed with thermal field emission spectroscopy. *Appl Phys Lett* 1999;75(18):2773–5.
- [34] Baker FS, Osborn AR, Williams J. The carbon-fibre field emitter. *J Phys D* 1974;7:2105–15.